

## SOLPS simulations for alternative divertor configurations in the future upper divertor in ASDEX Upgrade

O. Pan<sup>1</sup>, T. Lunt<sup>1</sup>, M. Wischmeier<sup>1</sup>, D. Coster<sup>1</sup>, U. Stroth<sup>1,2</sup> and the ASDEX Upgrade Team

<sup>1</sup> Max-Planck-Institut für Plasmaphysik, Boltzmannstr. 2, 85748 Garching, Germany

<sup>2</sup> Physik-Department E28, Technische Universität München, 85747 Garching, Germany

High heat loads on the divertor targets impose severe constraints on the achievable performance of future fusion reactors, e.g. DEMO [1]. In order to investigate possible solutions for the power exhaust problem, ASDEX Upgrade (AUG) has planned an upgrade of its upper divertor [2] to study alternative divertor configurations, e.g. the snowflake divertor (SF) [3] and the X-divertor (XD) [4]. Recently, the transport code SOLPS [5, 6] was successfully applied to simulate the alternative divertor configurations in the future upper divertor in AUG [7, 8]. In these simulations, the transport coefficients were assumed spatially constant. However, a precise fit to experimental measurements requires spatially varying transport coefficients, especially for H-mode discharges with a transport barrier at the edge of the confinement region. In this work, radially varying transport coefficients were used in the SOLPS-ITER simulations to reproduce the experimental conditions and to predict the performance of the future upper divertor of AUG.

### Experiments and simulations setup

In AUG, a series of single null H-mode discharges were carried out to prepare the upper divertor upgrade and used for the comparison with SOLPS-ITER simulations. The experiment was carried out with a plasma current of  $I_p = 0.8$  MA and a toroidal magnetic field of  $B_T = +2.5$  T ( $\vec{B} \times \nabla B$  ion drift pointed to the upper divertor). The time evolution of the main plasma parameters is shown in Fig. 1. The ECRH power was constant at 2.5 MW during the entire flat-top phase, and the NBI heating power was ramped in three steps to 2.5, 5.0 and 7.5 MW as shown in Fig. 1 (b). The deuterium was fueled from the lower divertor roof baffle at the

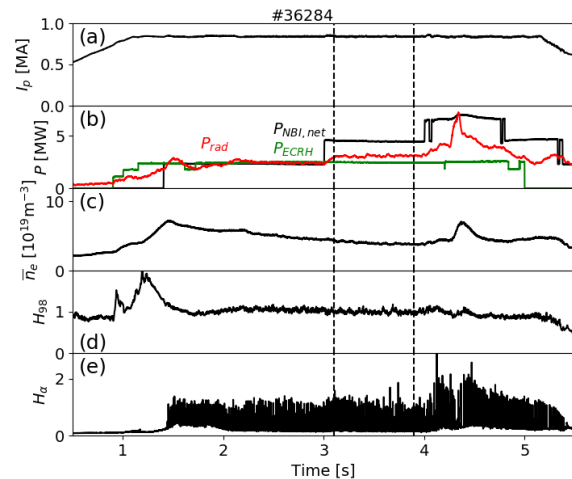


Figure 1: Time evolution of (a) plasma current, (b) heating and radiation power, (c) core line integrated density, (d)  $H_{98}$  confinement factor and (e)  $H_{\alpha}$  emission measured by the fast camera.

beginning of the discharge. The main impurity was nitrogen, puffed in previous discharges that remained in the machine. The confinement factor  $H_{98} \approx 1$  and type-I ELMs visible in the  $H_\alpha$  emission signals indicate that the discharge was in H-mode. The stable time phase from 3.1 s to 3.9 s was chosen for comparison with SOLPS-ITER simulations.

Figure 2 (a) and (b) show the electron density and temperature profiles mapped to the outer mid-plane (OMP). The electron density and temperature were measured by Thomson Scattering (CTS, ETS), Electron Cyclotron Emission Radiometry (ECE) and Helium Beam emission spectroscopy (HEB). The profiles calculated by the Integrated Data Analysis (IDA) [9], a tool coherently combining several diagnostics, are also shown for reference. Figure 2 (c) and (d) show the electron temperature and ion saturation current measured by Langmuir Probes (LPs) at the outer target. Figure 3 shows the target power flux measured by Infrared Camera (IR) averaging over time intervals containing ELMs.

Both targets were attached. In the SOLPS-ITER simulations, the computational grids were generated based on the experimental equilibrium. The injection positions of D<sub>2</sub> and N<sub>2</sub> were the same as in the experiments. The coefficients of transport, boundary conditions and fueling/seeding in the simulations were adjusted iteratively to match the experimental measurements at both the outer mid-plane and the targets. The profiles reproduced by SOLPS-ITER are shown by the solid blue lines in Fig. 2 and Fig. 3.

### Extrapolation to the future upper divertor

With the same input parameters, the plasma conditions in the present single null configuration were extrapolated to those in the future single null, snowflake and X-divertor configurations to predict their performance. The power fluxes perpendicular to the target ( $q_\perp$ ) and the radiation power density are compared in Fig. 3 and Fig 4, respectively. In the future single null divertor, the poloidal angle between the divertor leg and the target plate is smaller compared to the present divertor, resulting in a larger plasma-wetted area and a slightly lower power flux at the targets.

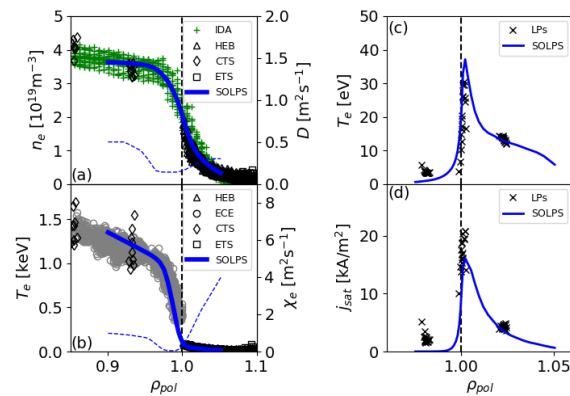


Figure 2: Outer mid-plane profiles of (a) electron density, (b) electron temperature and outer target profiles of (c) electron temperature, (d) ion saturation current. The solid and dashed curves show the profiles reproduced by SOLPS and the transport coefficients used in the simulations, respectively.

In the snowflake case, the electron density is higher in the confinement region compared to the single null case, while the profiles of electron and ion temperatures are found to be similar in these two configurations. The two nearby X-points in the snowflake configuration modify the magnetic pitch angle and may influence the particle transport [3]. At the outer target, the snowflake case shows substantially higher density and lower temperature compared to the single null case. A region with high density, low temperature and high radiation rate forms near the primary X-point (see Fig. 4 (d)), similar to the X-point radiator found in the lower single null experiments in AUG and JET [10]. As a result, the power fluxes are reduced by about one order of magnitude at both inner and outer targets compared to the single null case (see Fig. 3). The temperature at the target is around 1 eV, which is typical for detached divertor conditions. The smaller magnetic pitch angle near the X-points in the snowflake configuration could facilitate the maintenance of the strong poloidal temperature gradient near the radiator. This could also be an attractive benefit of the snowflake divertor configuration and is foreseen to be tested in future experiments.

In the X-divertor case, the simulation predicts higher electron densities at the outer mid-plane comparing to the single null case with the same transport coefficients and gas puffing rates. Different from the snowflake case, the density in the X-divertor case is higher not only in the confinement region but also in the SOL. Since the fueling rates are kept the same, the additional particle source for the higher density in the SOL is the ionization of the recycling particles. At the outer target, the maximum electron density is more than one order of magnitude higher than that in the single null case. This is a result of the combination of the higher up-stream density and the effect of the divertor con-

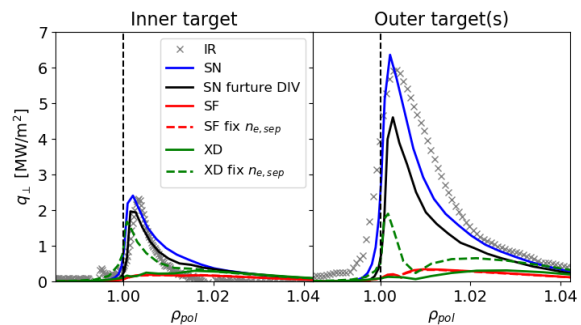


Figure 3: Power flux perpendicular to the inner (left) and outer (right) target from IR measurements in SN experiment and SOLPS simulations in SN, XD and SF configurations.

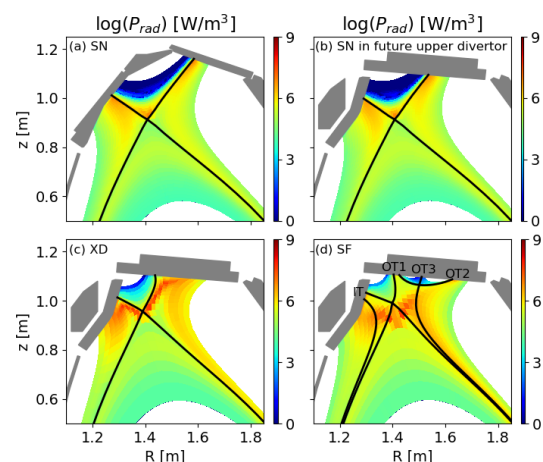


Figure 4: Radiation power density in SN with the (a) present and (b) future divertor targets and in (c) XD and (d) SF configurations.

figuration. Compared to the single null case, the maximum power fluxes shown in Fig. 3 are reduced by factors of 7 and 15 at the inner and outer targets, respectively.

In order to exclude the influence of the enhanced upstream density, the transport coefficients and fueling rates in the above snowflake and X-divertor cases were modified to achieve similar separatrix densities as those in the single null case. The results are shown by the dashed lines in Figs. 3. Comparing the two snowflake cases, no significant change is found at the target. This means that the different divertor conditions in the single null and snowflake simulations are not caused by the higher density in the confinement region. In the X-divertor case with fixed separatrix density, the density and ionization rates in the divertor are both lower compared to the above X-divertor case, resulting in lower power dissipation. The power fluxes are higher than those in the above X-divertor case but still lower than those in the single null case. The maximum temperature at the outer target is similar to that in the single null case, showing an attached outer target. This implies that the capacity of power dissipation in the X-divertor configuration is more sensitive to the upstream conditions.

## Summary

In this work, the SOLPS-ITER code package was applied to predict the plasma conditions in the alternative divertor configurations in the future upper divertor in AUG. The transport coefficients, boundary conditions and gas puffing rates in the simulations are selected to reproduce the experimentally measured profiles in dedicated upper single null H-mode discharges in AUG. Using the same input parameters, the plasma conditions in the single null case were then extrapolated to those in the snowflake divertor and the X-divertor configurations. The simulation showed much lower target power fluxes and a detached divertor in these alternative divertor configurations while the divertor in the single null reference is still attached. The alternative divertor configurations thus show an advantage in solving the power exhaust problem.

## References

- [1] H. Zohm *et al.*, Nucl. Fusion **53**, 073019 (2013)
- [2] T. Lunt *et al.*, Nucl. Mat. Energy **12**, 1037–1042 (2017)
- [3] D. Ryutov and V. Soukhanovskii, Phys. Plasmas **22**, 110901 (2015)
- [4] M. Kotschenreuther *et al.*, Phys. Plasmas **14**, 072502 (2007)
- [5] R. Schneider *et al.*, Contrib. Plasma Phys. **46**, 3–191 (2006)
- [6] S. Wiesen *et al.*, J. Nucl. Mater. **463**, 480–484 (2015)
- [7] O. Pan *et al.*, Plasma Phys. Control. Fusion **60**, 085005 (2018)
- [8] O. Pan, Doctoral dissertation, Technische Universität München (2020)
- [9] R. Fischer *et al.*, Fusion Sci. Technol. **58**, 675 (2010)
- [10] M. Bernert *et al.*, Nucl. Mat. Energy **12**, 111–118 (2017)